

Organic and Biological Chemistry

Studies on Models for Tetrahydrofolic Acid. II. Additional Observations on the Mechanism for Condensation of Formaldehyde with Tetrahydroquinoxaline Analogs

Stephen J. Benkovic,¹ Patricia A. Benkovic, and Robert Chrzanowski

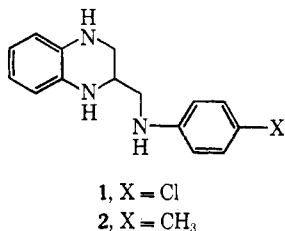
Contribution from the Department of Chemistry, The Pennsylvania State University, University Park, Pennsylvania 16802. Received May 22, 1969

Abstract: The condensation of formaldehyde with additional tetrahydroquinoxaline model systems in which the basicity of the exocyclic amino group has been varied through alterations in *para* substitution has been studied. Supporting evidence for a mechanism involving general base catalysis of attack by the exocyclic amino group on the iminium cation to yield the imidazolidine adduct is derived from these investigations. Experiments with a similar tetrahydroquinoline model indicate the importance of the nitrogen-8 of the tetrahydropyrazine ring on the rate of acid-catalyzed dehydration of the intermediate carbinolamine. The implication of these results as to the mechanism of action of the natural cofactor is discussed.

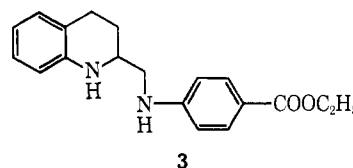
In a previous paper we have discussed the condensation of formaldehyde with a tetrahydroquinoxaline derivative, ethyl *p*-[N'-2'-(1,2,3,4)-tetrahydroquinoxalinylmethylene]aminobenzoate, as a possible model system for the tetrahydrofolic acid-5,10-methylene-tetrahydrofolic acid interconversion. The evidence suggested the presence of a steady-state intermediate interpreted as an iminium cation, which would function as a reactive species in the transfer of a one-carbon unit at the level of oxidation of formaldehyde. An important question, which could only be tentatively answered owing to the complication of kinetic indistinguishability, is whether catalysis occurs in the formation of the iminium cation or in the step leading to ring closure. In this paper our studies are extended in order to explore this problem and to further elucidate the function of various features of the natural cofactor.

Results and Discussion

The syntheses of the tetrahydroquinoxaline derivatives **1** and **2** were by methods previously described.² The structures of the tetrahydroquinoxalines and the corresponding imidazolidine adducts formed upon con-



densation with formaldehyde were assigned on the basis of spectral arguments discussed earlier. The synthesis of the tetrahydroquinoline model **3** commenced with quinoline-2-aldehyde followed by Schiff base formation



and reduction. Treatment of the anil with sodium borohydride in methanol yielded only the product of hydrogenation of the exocyclic azomethine bond, ethyl *p*-(2-quinolinylmethylene)aminobenzoate. Catalytic hydrogenation (PtO₂-ethanol) gave the desired tetrahydroquinoline **3**, deduced on the basis of the following evidence. The integrated nmr spectrum in CDCl₃ shows a doublet at δ 7.9 (2 H, aromatic), a complex multiplet centered at δ 6.4 (6 H, aromatic), a singlet at δ 4.2 (2 H-N), a quartet at δ 4.3 (2 H, CO₂CH₂-), a complex multiplet centered at δ 3.5 (H-C-H, methine), an unsymmetrical doublet at δ 3.2 (2 HC-N, methylene), two complex multiplets at δ 2.6-3.0 and 1.6-2.1 (2 H α and 2 H β to C₆H₄), and a triplet at δ 1.35 (CO₂CH₂CH₃). The ultraviolet spectrum reveals two long-wavelength absorption bands ($\lambda_{\text{max}}^{\text{ether}}$) at 297 (ϵ 33,700) and 253 m μ (ϵ 17,200). Compound **3** ionizes to give a mass spectrum fragmentation pattern with a parent ion (m/e 310, theoretical m/e 310) and shows the expected infrared absorption of N-H at 3300-3400 cm⁻¹. Condensation of **3** with formaldehyde yields the imidazolidine adduct whose structure is consistent with spectral and analytic data (see Experimental Section). A distinguishing feature is the appearance of N-CH₂-N absorption in the nmr spectrum (CD₃Cl) as an AB quartet, δ 4.6 (J_{ab} = 4.0 cps). The geminal coupling constant is characteristic of ring size and has been utilized in assigning structure in the tetrahydroquinoxaline series.

The pseudo-first-order rate constants, k_{obsd} , for the rate of formation of the formaldehyde adducts from **1** and **2** were determined spectrophotometrically from the time-dependent increase in absorbance at 260 and 310 m μ , respectively (solvent 50% v/v dioxane-H₂O, μ = 0.2, 25°). In the case of **1** and **2**, k_{obsd} changes from

(1) National Institutes of Health Career Development Awardee, Alfred P. Sloan Fellow, 1968-1970.

(2) S. J. Benkovic, P. A. Benkovic, and D. R. Comfort, *J. Amer. Chem. Soc.*, **91**, 5270 (1969).

Table I

Substrate	pK_a'	k_1 ($M^{-1} \text{ min}^{-1}$)	$k_3'K_{WD}k_1/(k_3 + k_{-1})$, min^{-1}	$k_3k_1/(k_3 + k_{-1})$, $M^{-1} \text{ min}^{-1}$	k_0 , min^{-1}
1	4.48 ± 0.1^a 1.46 ± 0.1^a	7.50×10^5 ^d	9.0×10^{-8} ^d	1.0×10^5 ^d	
2		3.16×10^6 ^d			
3	2.58 ± 0.03^b -1.10 ± 0.05^c	1.80×10^{-1} ^e			1.20×10^{-2} ^e

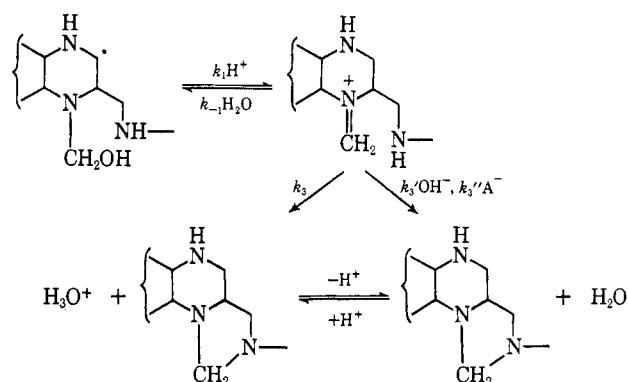
^a Determined spectrophotometrically at 240 m μ , H₂O, 25°, $\mu = 0.2$ for higher pK_a . ^b Determined spectrophotometrically at 250 m μ , 50% v/v dioxane-water, $\mu = 0.2$, 25°. ^c Determined spectrophotometrically at 300 m μ , H₂O, 25°. ^d The values of experimental rate constants assigned to the rate constants of Scheme I employing reiterative procedures ($\pm 15\%$). ^e The values assigned k_0 and k_1 of eq 4.

first order to zero order in formaldehyde concentration as the latter is varied, identical in behavior with that found for the *p*-carboethoxytetrahydroquinoxaline derivative. The equilibrium constants (K_1)^{3a} determined as the negative of the abscissa intercepts of double reciprocal plots of k_{obsd} vs. $[\text{CH}_2(\text{OH})_2]$ ^{3b} are $6.0 \times 10^3 M^{-1}$ and $4.5 \times 10^3 M^{-1}$ for 1 and 2 at pH values where the substrates are effectively in the free base form. These values compare favorably with an average $K_1 = 5.5 \times 10^3 \pm 1.1 M^{-1}$ for the *p*-carboethoxy-substituted tetrahydroquinoxaline model and are subject to a similar interpretation, that is, carbinolamine formation at the ring nitrogens. The above equilibrium constants when corrected by a factor of two for the reduced activity of water in the mixed solvent fall within a range characteristic of secondary cyclic amines (76 – $1600 M^{-1}$) and are to be compared to values of 2 – $40 M^{-1}$ for formaldehyde affinity of acyclic secondary amines.⁴ The large differences in K_1 between various amine types (primary, secondary, cyclic, etc.) has been attributed to steric effects on carbinolamine stability since K_1 is nearly insensitive to amine pK_a .⁴ The above values, however, probably also include binding of formaldehyde at the kinetically unproductive N-4 of the model substrates but not to any measurable extent at the exocyclic amino group owing to an absence of inhibition in k_{obsd} at high formaldehyde concentrations. Experiments designed to study k_{obsd} as a function of pH for substrates 1 and 2 were conducted at saturating formaldehyde of $1.47 \times 10^{-3} M$ where k_{obsd} is experimentally independent of formaldehyde concentration and the kinetics are pseudo first order [1 and $2 \cong 3.0 \times 10^{-4}$ – $3.0 \times 10^{-5} M$]. The rapid formation of carbinolamine is also detected by the lag phase at early times in the plots of $\log (\text{OD}_\infty - \text{OD}_t)$ against time employed to calculate k_{obsd} .

The pH-rate profiles for k_{obsd} at saturating formaldehyde concentration for 1 and 2 extrapolated to zero buffer concentration are presented in Figure 1. In contrast to the nonlinear behavior observed with the *p*-carboethoxy analog, the above profile for the model compound with *p*-CH₃ substitution may be satisfactorily rationalized in terms of simple acid-catalyzed dehydration of a carbinolamine intermediate leading to ring closure. In the case of *p*-Cl substitution the behavior of k_{obsd} as a function of pH resembles the *p*-COOC₂H₅ model with the dominance of the pH-independent region being restricted to a narrower range of

acidity. Moreover buffer catalysis is nearly negligible in the case of 1 and not detectable for 2. This finding for 2 is in accord with numerous investigations of acid-catalyzed dehydration of carbinolamines which proceed almost entirely through hydronium ion catalysis (Brønsted $\alpha = 0.7$ – 0.9).⁵ The values assigned to the rate constants of Scheme I (see below) for 1 and 2 based

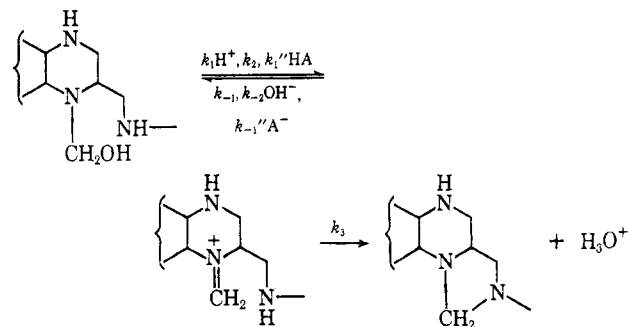
Scheme I



on these measurements and the pK_a values for 1 are tabulated in Table I.

In our preceding paper two schemes were proposed to explain the unique features of the pH-rate profile encountered in the conversion of the carbinolamine to the imidazolidine adduct when the exocyclic amino group was derived from *p*-carboethoxyaniline (Figure 1). Both Schemes I and II generate the observed kinetic de-

Scheme II



pendence of k_{obsd} —extrapolated to zero buffer and at saturating formaldehyde concentration—on pH (Figure 1, *p*-COOC₂H₅) yielding with the assumption of a steady-state iminium cation the general equation

$$k_{\text{obsd}} = \frac{(\text{AH}^+ + \text{B})\text{H}^+}{\text{H}^+ + \text{C}} \quad (1)$$

(3) (a) The equilibrium constant (K_1) is defined as the ratio [carbinolamine]:[1 or 2][CH₂(OH)₂] and has the units M^{-1} ; (b) formaldehyde is nearly entirely hydrated in aqueous solution, but its rate of dehydration to free formaldehyde would not be rate controlling under the above conditions (P. LeHenaff, *Compt. Rend.*, **256**, 1752 (1963)).

(4) R. G. Kallen and W. P. Jencks, *J. Biol. Chem.*, **241**, 5864 (1966).

(5) K. Koehler, W. Sandstrom, and E. H. Cordes, *J. Amer. Chem. Soc.*, **86**, 2413 (1964), and references therein.

Identifying the parametric values with Scheme I leads to the following equation for k_{obsd}

$$k_{\text{obsd}} = \left[\frac{\frac{k_3 k_1}{(k_{-1} + k_3)} \text{H}^+ + \frac{k_3' K_{\text{WD}} k_1}{(k_{-1} + k_3)}}{\text{H}^+ + \frac{k_3' K_{\text{WD}}}{(k_{-1} + k_3)}} \right] \text{H}^+ \quad (2)$$

or in the case of Scheme II gives

$$k_{\text{obsd}} = \left[\frac{\frac{k_3 k_1}{(k_{-1} + k_3)} \text{H}^+ + \frac{k_3 k_2}{(k_{-1} + k_3)}}{\text{H}^+ + \frac{K_{-2} k_{\text{WD}}}{(k_{-1} + k_3)}} \right] \text{H}^+ \quad (3)$$

where K_{WD} is defined as the autoprotolysis constant of H_2O in 50% v/v dioxane- H_2O .

In the case of Scheme I for the $p\text{-COOC}_2\text{H}_5$ model reaction the three main features of the pH-rate profile arise as follows: (1) pH 3.5–4.5; $\text{AH}^+ > \text{B}$ and $\text{H}^+ \gg \text{C}$, with $k_{\text{obsd}} = k_3 k_1 \text{H}^+ / (k_{-1} + k_3)$; (2) pH 5.5–7.0; $\text{B} > \text{AH}^+$ and $\text{H}^+ > \text{C}$ with $k_{\text{obsd}} = k_3' K_{\text{WD}} k_1 / (k_{-1} + k_3)$; and (3) pH 8.0–9.0; $\text{B} \gg \text{AH}^+$ and $\text{C} > \text{H}^+$ with $k_{\text{obsd}} = k_1 \text{H}^+$. Scheme I, therefore, may be analyzed in terms of rate-determining transitions from water to base-catalyzed ring closure and ultimately rate-determining acid-catalyzed dehydration with increasing pH. Following the same reasoning with Scheme II indicates that the pH-profile is generated as follows: (1) pH 3.5–4.5; $k_{\text{obsd}} = k_3 k_1 \text{H}^+ / (k_{-1} + k_3)$; (2) pH 5.5–7.0; $k_{\text{obsd}} = k_3 k_2 / (k_{-1} + k_3)$; and (3) pH 8.0–9.0; $k_{\text{obsd}} = k_3 k_2 \text{H}^+ / k_{-2} K_{\text{WD}}$. The above assumptions for the relative magnitudes of the parametric values impose an additional restriction on the description of the pH-rate profile in terms of Scheme II, namely $k_3 \gg k_{-1}$, so as not to violate the principle of microscopic reversibility. Consequently in the pH region 3.5–4.5, $k_{\text{obsd}} = k_1 \text{H}^+$ and pH 5.5–7.0, $k_{\text{obsd}} = k_2$. In the case of Scheme II the profile, therefore, results from changes in the rate-determining step from acid-catalyzed to spontaneous dehydration of carbinolamine and ultimately ring closure with increasing pH. From the above it is obvious that in order to generate the pH-rate profile for the $p\text{-COOC}_2\text{H}_5$ model reaction, opposing assumptions are required concerning the magnitude of k_3 and k_1 , i.e., for Scheme I $k_{-1} \gtrless k_3$ whereas for Scheme II $k_{-1} \ll k_3$.

The question now arises as to the effect of a change in the nature of the *para* substituent on the values of k_3 , k_3' , and k_{-1} . Intuitively increased electron donation by a *para* group which increases the basicity of the exocyclic nitrogen should affect primarily the values of k_3 and k_3' with the magnitude of k_3 increasing with increasing basicity, although the proportionality constant, β , is unknown.⁶ The value of k_3' (hydroxide ion catalyzed ring closure) should decrease with increasing amino group basicity as the requirement for catalysis diminishes although the extent of this change is also unknown. The magnitude of k_{-1} should remain nearly invariant to changes in *para* substitution. Small perturbations in k_{-1} owing to inductive or field effects would act to decrease the value of k_{-1} as the substituent becomes increasingly electron donating, i.e., increases the stability of the

(6) Insofar as it is applicable, nucleophilic attack by weakly basic amines on the ester carbonyl of *p*-nitrophenyl acetate under conditions in which the rate-determining step involves amine attack has been correlated with a β of 0.8: T. C. Bruice and R. Lapinski, *J. Amer. Chem. Soc.*, **80**, 2265 (1958); W. P. Jencks and J. Carriuolo, *ibid.*, **82**, 1778 (1960).

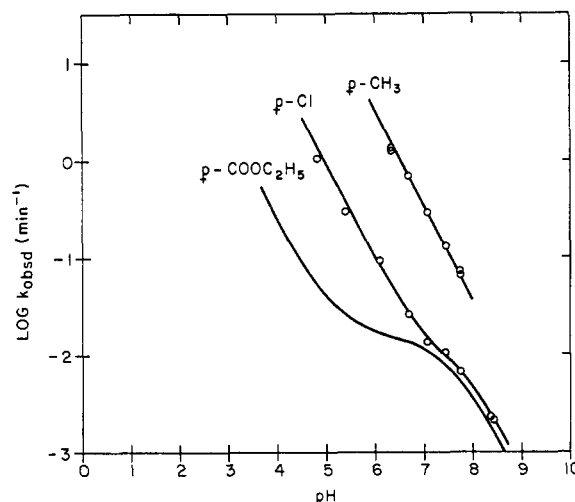


Figure 1. Graph of $\log k_{\text{obsd}}$ for the corresponding tetrahydroquinoxaline models extrapolated to zero buffer concentration against pH, $\mu = 0.2$, 25° , 50% v/v dioxane-water (k_{obsd} at saturating formaldehyde concentration extrapolated to zero buffer).

charged iminium cation relative to its more diffusely charged transition state for hydration. A complication in the above analysis for k_{-1} is the possibility that hydration of the iminium cation may be general base catalyzed by the neighboring amino group in which case k_{-1} would increase with increasing exocyclic nitrogen basicity. Effects arising from intramolecular catalysis can be reasonably discounted on the basis that the hydrolyses of protonated imines of weakly basic amines (benzylideneanilines) exhibit small sensitivity to the pK_a of the general base ($\beta = 0-0.2$)⁵ which in comparing the $p\text{-CH}_3$ and $p\text{-COOC}_2\text{H}_5$ models would result in a maximal change of only fivefold in the magnitude of k_{-1} . In summary the largest changes may be anticipated in the values of k_3 and k_3' .

The following is an analysis of the anticipated changes in the kinetic descriptions of Schemes I and II resulting from alterations in *para* substitution. (1) $k_3 \gg k_{-1}$. Scheme I reduces at all pH values to simply $k_{\text{obsd}} = k_1 \text{H}^+$, i.e., the pH-rate profile exhibits a linear dependence on hydronium concentration and is identified with acid-catalyzed dehydration of the carbinolamine. The magnitude of k_1 like k_{-1} should be nearly invariant to changes in *para* substitution although a trend to higher values may arise with electron-donating substituents owing to an increase in the stability of the cationic iminium transition state relative to carbinolamine. Scheme II remains as described above with the term $k_2 k_3 / k_{-2} K_{\text{WD}}$, associated with rate-determining ring closure dominating at higher pH values with increasing exocyclic amino group basicity. Increases in the equilibrium constant, $k_2 / k_{-2} K_{\text{WD}}$, should parallel the anticipated greater stabilization of the iminium cation relative to carbinolamine, and in conjunction with parallel effects on k_3 increase the magnitude of the above term. (2) $k_{-1} \gg k_3$. Scheme I remains as described above with the term for rate-determining ring closure, $k_1 k_3 / k_{-1}$, dominating at higher pH values with increasing exocyclic amino group basicity. (Note that dynamic equilibrium requires $k_1 / k_{-1} = k_2 / k_{-2} K_{\text{WD}}$.) Scheme II reduces at all pH values to simply $k_{\text{obsd}} = k_3 k_1 \text{H}^+ / k_{-1}$ and is identified with rate-determining ring closure. In summary both schemes can generate simpler pH-rate

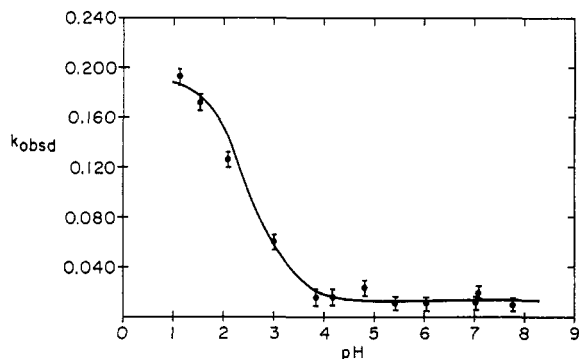


Figure 2. The pH-rate profile for the condensation of formaldehyde with **3** extrapolated to zero buffer concentration, $\mu = 0.2$, 25° , 50% v/v dioxane-water, $[\text{CH}_2(\text{OH})_2] = 1.47 \times 10^{-3} M$.

profiles where k_{obsd} is directly proportional to hydrogen ion concentration with the magnitude of the associated rate constant (either k_1 for Scheme I or $k_3 k_2 / k_{-2} K_{\text{WD}}$ for Scheme II) being equal to or greater than the same terms for the kinetics of the $p\text{-COOC}_2\text{H}_5$ model reaction described by the respective schemes.

Inspection of Figure 1 reveals that the rate constant associated with the low pH-dependent section of the profile appears to increase in magnitude in the order $p\text{-COOC}_2\text{H}_5 < p\text{-Cl} < p\text{-CH}_3$ resulting in the gradual disappearance of the complex behavior associated with the $p\text{-COOC}_2\text{H}_5$ model. Also recall that the magnitude of buffer catalysis is diminishing in the same order. This behavior parallels an increase in the basicity of the exocyclic amino group, since pK_a values attributed mainly to dissociation of the exocyclic nitrogen decrease in the order -0.33 ($p\text{-COOC}_2\text{H}_5$) < 1.46 ($p\text{-Cl}$) $< ca. 3.1$ ($p\text{-CH}_3$). The latter pK_a is estimated from the ΔpK_a of toluidine and p -chloroaniline adjusted to the model systems. These observations can be rationalized in terms of Scheme I where the greater sensitivity of k_3 relative to k_{-1} to alterations in *para* substitution results in $k_{-1} \gg k_3$ ($p\text{-COOC}_2\text{H}_5$) but $k_3 \gg k_{-1}$ ($p\text{-CH}_3$). Consistent with the operation of Scheme I are the following results derived on this basis: (1) the values attributed to the hydronium ion catalyzed dehydration of carbinolamines (k_1 , $M^{-1} \text{ min}^{-1}$) are 4.23×10^5 ($p\text{-COOC}_2\text{H}_5$), 7.50×10^5 ($p\text{-Cl}$), and 3.16×10^6 ($p\text{-CH}_3$) which are constant within an order of magnitude and are subject to electronic perturbations in the anticipated direction; (2) the decrease in the magnitude of catalysis associated with ring closure with increasing basicity;⁷ and (3) an *ca.* 40-fold increase in the value for rate-determining ring closure ($k_3 k_1 / k_{-1} + k_3$) for the $p\text{-Cl}$ relative to the $p\text{-COOC}_2\text{H}_5$ model reaction. The unlikely possibility that $k_{-1} \gg k_3$ with increasing exocyclic nitrogen basicity and that acid-catalyzed dehydration is subject to large electronic effects militates against Scheme II—the ratio of k_1 for the $p\text{-Cl}$ to the $p\text{-COOC}_2\text{H}_5$ model reaction is *ca.* 40-fold on this basis. Thus the available evidence strongly supports our earlier contention² that catalysis occurs in the ring closure step.

The pseudo-first-order rate constant (k_{obsd}) for formation of the formaldehyde adduct from the tetrahydroquinoline model **3** was also determined spectrophotometrically from the time-dependent increase in

absorbance at $310 \text{ m}\mu$ (solvent 50% v/v dioxane- H_2O , $\mu = 0.2$, 25°). In marked contrast to the tetrahydroquinoxaline models the kinetics remain first order in formaldehyde as the latter is varied from 0 to 1.84×10^{-3} – $3.68 \times 10^{-2} M$ over the pH range 2–8. The pH-rate profile, determined at constant formaldehyde concentration ($1.47 \times 10^{-3} M$) and zero buffer concentration, is presented in Figure 2. The experimental points can be described by the following equation

$$k_{\text{obsd}} = k_0 + \frac{k_1 \text{H}^+}{K_a + \text{H}^+} \quad (4)$$

where k_0 represents the water-catalyzed addition of formaldehyde and k_1 the water-catalyzed addition of formaldehyde to the monoprotonated form of **3**.⁸ The latter term may also be viewed as the kinetically indistinguishable acid-catalyzed addition of formaldehyde to the free base form of **3**. The present data are insufficient to resolve this point although in analogy with the condensation of formaldehyde with tetrahydrofolic acid the reaction may be described in terms of solvated proton acting as a general acid catalyst.⁹ From the observed buffer catalysis (acetate and formate) the value of the Brønsted α is 0.1–0.2 in the mixed solvent and therefore closely approximates the situation for general acid catalysis ($\alpha = 0.23$) of the attack of tetrahydrofolic acid on formaldehyde under similar conditions (H_2O , $\mu = 1.0$, 25°). The low value of α is also in accord with general-acid-catalyzed additions of other weakly basic amines to formaldehyde in more aqueous media.¹⁰ The inability to detect saturation kinetics at pH values < 8 (the extension to higher pH being limited by experimental considerations) demands that the acid-catalyzed dehydration for the presumed carbinolamine intermediate is $> 10^7 M^{-1} \text{ min}^{-1}$. Thus replacement of the N-4 of the tetrahydroquinoxaline models with a methylene unit serves to increase the rate of acid-catalyzed dehydration by a minimal factor of 10^2 .

The above discussion has several important implications concerning the mechanism of action of the natural cofactor. It is apparent that the ΔpK_a between N-5 and N-10 partially determines the lifetime of the iminium cation intermediate (k_3 and k_3') and controls the nature of the catalysis for imidazolidine formation or the converse ring opening. The observation and probable identification of general base catalysis in imidazolidine formation suggest a general-acid-catalyzed mode of ring opening, an attractive pathway for a biochemical process. Ring opening can be viewed as a balance between two discrete but thermodynamically opposing steps: (1) protonation at the least basic nitrogen *via* a thermodynamically unfavorable equilibrium; and (2) expulsion of the more acidic protonated amine in order to yield the thermodynamically more stable iminium cation at the more basic amino site. This description should not be construed to mean that the actual mechanism is a stepwise process: the Brønsted β (0.65) for the p -carboethoxytetrahydroquinoxaline model is suggestive of a concerted mechanism. The above description, however, implies that a discrete value of ΔpK_a will

(8) The lack of saturation in k_{obsd} by increasing formaldehyde concentrations results in alternate explanations being ambiguous, *i.e.*, the kinetics do not demand an iminium cation intermediate.

(9) R. G. Kallen and W. P. Jencks, *J. Biol. Chem.*, **241**, 5851 (1966).

(7) A quantitative comparison is prone to large error owing to the small contribution of these terms. However, $k_3' K_{\text{WD}} / (k_3 + k_{-1})$ for the $p\text{-COOC}_2\text{H}_5$ model reaction is 1.50×10^{-2} vs. 9.0×10^{-3} for $p\text{-Cl}$.

(10) L. do Amaral, W. A. Sandstrom, and E. H. Cordes, *J. Amer. Chem. Soc.*, **88**, 2225 (1966).

be associated with maximal cofactor efficiency in one-carbon unit transfers since (a) too small a ΔpK_a would require specific acid catalysis for ring opening because proton transfer should nearly be complete in order to sufficiently increase the acidity of the amino group for expulsion, and (b) too large a ΔpK_a would result in the equilibrium favoring formaldehyde or carbinolamine with the result that neither situation would be attractive for a biochemical process. The interesting observation that the rate of acid-catalyzed dehydration of carbinolamine is regulated by the nature of the atom at the 4-position of the heterocyclic ring mandates that the rate of hydration (k_{-1}) may be affected and thus has a direct bearing on the lifetime or concentration of the iminium cation. The magnitude of this "ortho effect" which is at least of the order of 10^3 may arise from (a) ion-dipole interaction, the dipole of the substituent amino group destabilizing the transition state leading to the iminium cation, or (b) ion-ion interactions in the aforementioned transition state stemming from the zwitterion form of unproductive carbinolamine at N-4. The possibility of proton tautomerization to other basic sites¹¹ in order to reduce charge at N-8 results in k_1 (acid-catalyzed dehydration) for tetrahydrofolic acid to be closer in magnitude to that observed for **3**. In a future paper we will attempt to place these contentions on a quantitative footing.

Experimental Section

Materials. The preparation of quinoline-2-aldehyde was by the method of Kaplan,¹² mp 68–70° (lit.¹² mp 70°), with the exception that a twofold molar excess of selenium dioxide was employed.

Ethyl *p*-(N'-2'-Quinaldylidene)aminobenzoate. Dry benzene (40 ml), 5.2 g (0.03 mol) of quinoline-2-aldehyde, and 5.5 g (0.03 mol) of ethyl *p*-aminobenzoate were refluxed for 5 hr to give the theoretical amount of water (0.5 ml, 0.03 mol) collected in a Dean-Stark trap. The solution was evaporated to dryness *in vacuo* to give a yellow residue which was scratched to induce crystallization. Repeated fractional crystallization of the solid mass from ether gave two crops of crystals of total weight 6.4 g, mp 89° and 135°, respectively. Thin layer chromatography of the two crystal crops on silica G gel showed three components under ultraviolet light after development in 10:1 cyclohexane-ethanol. Two of the components were found to be ethyl *p*-aminobenzoate and quinoline-2-aldehyde by comparison with authentic samples. Fractional crystallization from ether-petroleum ether or benzene-petroleum ether was not successful. The ultraviolet spectrum in ether (λ_{\max} 333, 302, and 262 m μ) of the two crystal crops was nearly identical with the ultraviolet spectrum of an authentic sample of *p*-(N'-2'-quinaldylidene)aminobenzoic acid prepared by the method of Klosa;¹³ $\lambda_{\max}^{\text{tetrahydrofuran}}$ 335 (ϵ 7000), 302 (ϵ 9000), and 263 m μ (ϵ 25,000); mp 222–224° (lit. mp 222°). The two crystal crops were combined and used in the next step without further purification.

Ethyl *p*-(N'-2'-Quinolylmethylene)aminobenzoate. Sodium borohydride (0.6 g, 0.02 mol) was dissolved in 100 ml of absolute methanol and cooled to 0°. The crude Schiff base, ethyl-*p*-(N'-2'-quinaldylidene)aminobenzoate (3.0 g, 0.01 mol), was dissolved in 100 ml of absolute methanol and added slowly to the borohydride solution. The temperature of the mixture was raised to 25° for 3 hr with continuous stirring. The reaction mixture was acidified with acetic acid, diluted with 500 ml of water, made alkaline with sodium bicarbonate, and extracted three times with 100-ml portions of ether. The ether extracts were combined, dried over sodium sulfate, and evaporated to dryness giving a yellow residue. Thin layer chromatography of the yellow residue on silica G gel showed four components under ultraviolet light after developing in 10:1 cyclohexane-ethanol. Three of the components were found to be

the starting Schiff base, ethyl *p*-aminobenzoate, and 2-quinoline-carbinol by comparison with authentic samples. An infrared spectrum of the material revealed that the $>C=N-$ stretching at 1630 cm⁻¹ had disappeared and a secondary N-H stretching at 3400 cm⁻¹ had appeared. Fractional crystallization of the residue from ether-petroleum ether or benzene-petroleum ether was unsuccessful and the residue was used directly in the next step.

Ethyl *p*-(N'-2'-Tetrahydroquinolylmethylene)aminobenzoate. Platinum oxide (0.3 g) was suspended in 200 ml of absolute ethanol and reduced for 30 min at atmospheric pressure in a hydrogenation unit. To this suspension, a solution of 3.0 g (0.01 mol) of ethyl *p*-(N'-2'-quinolylmethylene)aminobenzoate in 25 ml of ethanol was added and the solution was hydrogenated for 15 hr. The theoretical amount of hydrogen (500 ml) was taken up and the reaction ceased. The solution was filtered to remove the catalyst and evaporated to dryness *in vacuo* giving a yellow oily residue. A small quantity of the yellow residue was triturated with ether until a white crystalline solid was formed. A seed crystal of the product was added to the above oil and chilled in a freezer until partial crystallization had occurred. The resulting white crystalline solid was removed by filtration and washed with cold ether and petroleum ether in order to remove the remaining nonsolidified material. The filtrate was used for the preparation of the imidazolidine adduct.

The white crystalline solid (0.8 g, 25.0%) mp 93–94°, $\lambda_{\max}^{\text{ether}}$ 297 (ϵ 33,700), 253 m μ (ϵ 9200), gave a positive silver mirror test with 2% ethanolic silver nitrate. Thin layer chromatography of the crystals on silica gel G in 10:1 cyclohexane-ethanol under ultraviolet light showed one component of R_f value 0.25. Infrared investigation revealed secondary N-H stretching at 3300–3400 cm⁻¹ and bending at 1510 cm⁻¹, carbonyl stretching of an aromatic ester at 1725 cm⁻¹, and aromatic absorbances at 1600, 1480, 1180, 1100, 1020, and 830 cm⁻¹. An nmr spectrum taken in CDCl₃ with tetramethylsilane as an internal standard revealed a doublet at 7.9 ppm (2 H), a complex multiplet centered at 6.8 ppm (6 H), a singlet at 4.25 ppm (2 H), a symmetrical quartet of $J = 7.0$ cps centered at 4.3 ppm (2 H), a complex multiplet centered at 3.5 ppm (1 H), an unsymmetrical doublet centered at 3.2 ppm (2 H), a complex multiplet centered at 2.6 ppm (2 H), a complex multiplet centered at 1.8 ppm (2 H), and a symmetrical triplet centered at 1.35 ppm (3 H).

Anal. Calcd for C₁₉H₂₂N₂O₂: C, 73.5; H, 7.10; N, 9.05. Found: C, 72.77; H, 7.05; N, 9.02.

Imidazolidine Adduct of **3.** The filtrate from the preparation of ethyl *p*-(N'-2'-tetrahydroquinolylmethylene)aminobenzoate was evaporated to a residue *in vacuo* which was then dissolved in 100 ml of absolute ethanol. To this solution, 0.6 g (0.01 mol) of 85% concentrated formaldehyde in 10 ml of absolute ethanol was added. The reaction mixture was refluxed for 3 hr and chilled in a freezer for 1 day. A white crystalline precipitate formed which was removed by filtration and washed with cold ethanol: yield 0.8 g (25%), mp 148–149°, $\lambda_{\max}^{\text{ether}}$ 301 m μ (ϵ 36,000). The product did not give a silver mirror test with 2% ethanolic silver nitrate. Thin layer chromatography of the crystals on silica gel G developed in 10:1 cyclohexane-ethanol under ultraviolet light showed one component of R_f value 0.70.

Infrared investigation revealed the absence of any N-H stretching. An nmr spectrum in CDCl₃ with tetramethylsilane as an internal standard revealed a doublet at 8.0 ppm (2 H), a complex multiplet centered at 6.8 (6 H), a symmetrical quartet of $J = 4.0$ cps centered at 4.6 (2 H), a symmetrical quartet of $J = 7.0$ cps centered at 4.3 (2 H), a complex multiplet centered at 3.7 (2 H), a complex multiplet from 3.2 to 2.8 (3 H), a complex multiplet centered at 2.0 (2 H), and a symmetrical triplet of $J = 7.0$ cps centered at 1.4 (3 H).

Anal. Calcd for C₂₀H₂₃N₃O₂: C, 74.60; H, 6.80; N, 8.70; mol wt, 322. Found: C, 74.4; H, 6.80; N, 8.60; mol wt, 322 \pm 1.

N'-2'-Quinoxalylmethylidene-*p*-chloroaniline. The above anil was prepared from quinoxaline-2-aldehyde and *p*-chloroaniline according to published procedures¹⁴ and recrystallized from ethanol, mp 174–175°. **Anal.** Calcd for C₁₅H₁₀N₂Cl: C, 67.29; H, 3.77; N, 15.70. Found: C, 66.8; H, 4.05; N, 15.68.

N'-2'-(1,2,3,4)-Tetrahydroquinoxalylmethylene-*p*-chloroaniline. The synthesis of the desired tetrahydroquinoxaline substrate was identical with that previously published; recrystallized from benzene-petroleum ether, mp 106–108°, $\lambda_{\max}^{\text{H}_2\text{O}}$ (pH 7) 252, 291 m μ . **Anal.** Calcd for C₁₅H₁₄N₂Cl: C, 65.81; H, 5.89; N, 15.35. Found: C, 65.6; H, 6.09; N, 15.17.

(11) The 3-amido function incorporated into the pyrimidine ring is ionized at pH values where k_1 is rate determining and is a potential proton acceptor site.

(12) H. Kaplan, *J. Amer. Chem. Soc.*, **63**, 2654 (1941).

(13) Josef Klosa, *Arch. Pharm.*, **177** (1956).

(14) C. L. Leese and H. N. Rydon, *J. Chem. Soc.*, **308** (1955); A. Kjaer, *Acta Chem. Scand.*, **2**, 456 (1948).

Imidazolidine Adduct of 1. The synthesis of the formaldehyde adduct was identical with previous published procedures; recrystallized from benzene-petroleum ether, mp 208–209°, λ_{max} (50% v/v dioxane-water) 260 (ϵ 28,135). *Anal.* Calcd for $\text{C}_{16}\text{H}_{18}\text{N}_2\text{Cl}$: C, 67.23; H, 5.65; N, 14.71. Found: C, 67.34; H, 5.81; N, 14.72.

All utilized kinetic procedures have already been described in ref 2.

Acknowledgment. This research was supported by Research Grant GB-7246 from the National Science Foundation.

Homogeneous Catalysts for Olefin Disproportionations from Nitrosyl Molybdenum and Tungsten Compounds

E. A. Zuech, W. B. Hughes, D. H. Kubicek, and E. T. Kittleman

Contribution from the Research and Development Department, Phillips Petroleum Company, Bartlesville, Oklahoma. Received June 2, 1969

Abstract: Homogeneous catalyst systems have been discovered which have effected the disproportionation of a variety of olefins. The catalysts are obtained from the reaction of nitrosyl molybdenum and tungsten derivatives with such organoaluminum compounds as $\text{C}_2\text{H}_5\text{AlCl}_2$ and $(\text{CH}_3)_3\text{Al}_2\text{Cl}_3$. Suitable group VIB element catalyst components include the known dichlorodinitrosylmolybdenum(II) and -tungsten(II) complexes or a large number of *in situ* preparations resulting from nitric oxide treatment. Among the possible olefin reactions are the conversion of 1-pentene to ethylene and 4-octene and the ethylene cleavage of 1,5-cyclooctadiene to give 1,5,9-decatriene.

The discovery of the olefin disproportionation process over heterogeneous catalysts^{1,2} has been the impetus for further exploratory investigations into this unique reaction.^{3,4} In a previous communication,⁵ combinations of nitrosyl molybdenum and tungsten compounds with organoaluminum halides were reported to give homogeneous catalysts which exhibited this unusual property. This article will more clearly define these soluble systems, as well as broaden the scope of their preparation and utility.

Soluble catalyst systems derived from $\text{WCl}_6\text{-Et-AlCl}_2$,^{6,7} $\text{WCl}_6\text{-EtOH-EtAlCl}_2$,^{6,7} and $\text{WCl}_6\text{-}n\text{-BuLi}^8 have recently been disclosed. The new catalysts described herein not only contain a number of different ligands but also specify the singular effectiveness of the nitrosyl ligand. In contrast to the above systems from WCl_6 ⁶⁻⁸ in which only internal olefins were satisfactory substrates, these nitrosyl-containing catalysts will effect disproportionation of α -olefins as well as ethylene-cleavage reactions.$

Treatment of the green nitrosyl complex, $[(\text{C}_6\text{H}_5)_3\text{P}]_2\text{-Cl}_2(\text{NO})_2\text{Mo}$,⁹ with $(\text{CH}_3)_3\text{Al}_2\text{Cl}_3$ in chlorobenzene at 0–5° resulted in a brown homogeneous solution. This was then treated with 1-pentene, under conditions wherein the ethylene formed could be vented at atmospheric pressure. Hydrolysis after 50 min followed by glpc analysis employing *n*-heptane as a standard indicated the presence of 48 mol % of 4-octene⁴ and 48 %

of unreacted 1-pentene; no additional products other than ethylene were detected. A comparable reaction mixture allowed to stand 21 hr at ambient temperature gave, upon analysis using a cyclohexane standard, 33 % of 1-pentene, 0.6 % of C_6 olefins, 0.6 % of C_7 olefins, and 61 % of 4-octene. This catalyst combination with 1-octene at 0–5° for 30 min afforded 7-tetradecene⁴ in 37 % yield.

In the above reactions, little isomerization of the olefins was detected. However, when $\text{C}_2\text{H}_5\text{AlCl}_2$ was used as the cocatalyst with the above molybdenum

Table I. Reactions with $[(\text{C}_6\text{H}_5)_3\text{P}]_2\text{Cl}_2(\text{NO})_2\text{Mo}$ and $\text{C}_2\text{H}_5\text{AlCl}_2$ ^a

	Reactant 1-Pentene	Products, wt % ^b 1-Octene
C_4H_8	18 (16 + 0) ^c	7
C_6H_{10}	25 (23 + 0.1)	2
C_6H_{12}	28 (27 + 0.1)	3
C_7H_{14}	11 (10 + 1.5)	8
C_8H_{16}	16 (18 + 0.1)	20
C_9H_{18}	^t	18
$\text{C}_{10}\text{H}_{20}$		3
$\text{C}_{11}\text{H}_{22}$		4
$\text{C}_{12}\text{H}_{24}$		9
$\text{C}_{13}\text{H}_{26}$		13
$\text{C}_{14}\text{H}_{28}$		12
$\text{C}_{15}\text{H}_{30}$		0.4

^a Both reactions were conducted utilizing 0.5 mmol of the molybdenum complex and 0.2 ml of $\text{C}_2\text{H}_5\text{AlCl}_2$ at ambient temperature for 16 hr. The 1-pentene reaction mixture contained 10 ml of the olefin and 10 ml of chlorobenzene, while the other system contained 20 ml of 1-octene and 20 ml of chlorobenzene. ^b Ethylene and propylene were present in both products but excluded from the calculations. ^c These percentages were obtained by glpc capillary column analysis of the hydrogenation product; the first number in each group refers to the linear product and the second to the branched material. ^d Traces of higher olefins were present.

compound, isomerization occurred to give a distribution of olefinic products (Table I). A comparison of the 1-pentene reaction with the above 1-pentene- $(\text{CH}_3)_3\text{-}$

(1) R. L. Banks and G. C. Bailey, *Ind. Eng. Chem. Prod. Res. Develop.*, **3**, 170 (1964).

(2) The terms "dismutation" and "metathesis" have also been employed to describe this reaction.

(3) C. P. C. Bradshaw, E. J. Howman, and L. Turner, *J. Catal.*, **7**, 269 (1967).

(4) D. L. Crain, *ibid.*, **13**, 111 (1969).

(5) E. A. Zuech, *Chem. Commun.*, 1182 (1968).

(6) N. Calderon, H. Y. Chen, and K. W. Scott, *Tetrahedron Lett.*, 3327 (1967).

(7) N. Calderon, E. A. Ofstead, J. P. Ward, W. A. Judy, and K. W. Scott, *J. Amer. Chem. Soc.*, **90**, 4133 (1968).

(8) J. L. Wang and H. R. Menapace, *J. Org. Chem.*, **33**, 3794 (1968).

(9) F. A. Cotton and B. F. G. Johnson, *Inorg. Chem.*, **3**, 1609 (1964).